Distinct Roles of PI(3,4,5)P3 during Chemoattractant Signaling in Dictyostelium

Loovers, Harriet; Postma, Marten; Keizer-Gunnink, Ineke; Huang, Yi Elaine; Devreotes, Peter N.; Haastert, Peter J.M. van

Published in:
Molecular Biology of the Cell

DOI:
10.1091/mbc.E05-09-0825

Publication date:
2006

Molecular Biology of the Cell
Vol. 17, 1503–1513, April 2006

Distinct Roles of PI(3,4,5)P_3 during Chemoattractant Signaling in *Dictyostelium*: A Quantitative In Vivo Analysis by Inhibition of PI3-Kinase[V]

Harriët M. Loovers,*† Marten Postma,*‡ Ineke Keizer-Gunnink,* Yi Elaine Huang,§ Peter N. Devreotes,§ and Peter J.M. van Haastert*

*Department of Molecular Cell Biology, University of Groningen, 9751NN Haren, The Netherlands; and §Department of Cell Biology, Johns Hopkins University School of Medicine, Baltimore, MD 21205

Submitted September 1, 2005; Revised December 8, 2005; Accepted January 9, 2005
Monitoring Editor: John York

The role of PI(3,4,5)P_3 in *Dictyostelium* signal transduction and chemotaxis was investigated using the PI3-kinase inhibitor LY294002 and *pi3k*-null cells. The increase of PI(3,4,5)P_3 levels after stimulation with the chemoattractant cAMP was blocked >95% by 60 μM LY294002 with half-maximal effect at 5 μM. This correlated well with the inhibition of the membrane translocation of the PH-domain protein, PHcracGFP. LY294002 did not reduce cAMP-mediated cGMP production, but significantly reduced the cAMP response up to 75% in wild type and completely in *pi3k*-null cells. LY294002-treated cells were round, not elongated as control cells. Interestingly, cAMP induced a time and dose-dependent recovery of cell elongation. These elongated LY294002-treated wild-type and *pi3k*-null cells exhibited chemotactic orientation toward cAMP that is statistically identical to chemotactic orientation of control cells. In control cells, PHcrac-GFP and F-actin colocalize upon cAMP stimulation. However, inhibition of PI3-kinases does not affect the first phase of the actin polymerization at a wide range of chemoattractant concentrations. Our data show that severe inhibition of cAMP-mediated PI(3,4,5)P_3 accumulation leads to inhibition of cAMP relay, cell elongation and cell aggregation, but has no detectable effect on chemotactic orientation, provided that cAMP had sufficient time to induce cell elongation.

INTRODUCTION

The ability to sense small differences in chemoattractant concentrations is essential for directed movement of eukaryotic cells, including neutrophils and the social amoeba *Dictyostelium discoideum*. Efficient chemotaxis requires a balanced interplay between several signal transduction pathways. One of these pathways is the regulated formation of myosin filaments at the uropod. In *D. discoideum*, myosin phosphorylation is regulated by the second messenger cGMP. Aberrant cGMP production influences lateral pseudopod formation and thereby chemotaxis efficiency (Bosgraaf *et al.*, 2002). Another pathway is the regulated actin polymerization at the leading edge, resulting in pseudopod formation at the front.

Production of the signaling molecule phosphatidylinositol-3,4,5-trisphosphate, PI(3,4,5)P_3, at the leading edge is implicated to regulate actin polymerization by localization of PH-domain containing proteins (Devreotes and Janetopoulos, 2003; Parent, 2004). The PH domain of CRAC translocates to the leading edge in response to this PI(3,4,5)P_3 production and mediates the production of cAMP (Parent *et al.*, 1998; Dormann *et al.*, 2004). Uniform stimulation of *D. discoideum* cells leads to activation of PI3-kinases and a transient PI(3,4,5)P_3 production is observed (Huang *et al.*, 2003). This transient increase in PI(3,4,5)P_3 levels is absent in *ddpik1/2*-null cells, a cell line with two PI3-kinases inactivated. Two groups of proteins negatively regulate PI(3,4,5)P_3 levels. The 3-phosphatase PTEN reverses the action of PI3-kinases, whereas inositol 5-phosphatases remove the phosphate group from the 5-position, producing PI(3,4)P_2. Inactivation of inositol 5-phosphatases does not negatively affect chemotaxis (Loovers *et al.*, 2003). In contrast, in *pten*-null cells both polarity and chemotaxis efficiency are reduced (Funamoto *et al.*, 2002; Iijima and Devreotes, 2002). In wild-type cells, PI3-kinases localize at the leading edge, whereas PTEN is excluded from this region (Funamoto *et al.*, 2002; Iijima and Devreotes, 2002). Cells with a deletion of *pten* exhibit elevated PI(3,4,5)P_3 levels in a broader front at the leading edge of the cell, which is associated with elevated levels of F-actin and the formation of many protrusions over a wide front. These observations strongly suggest a causal relationship between PI(3,4,5)P_3 production, actin assembly and pseudopod extension.

Cells with reduced PI3-kinase activity, either by deletion of two PI3-kinase genes or by inhibition of PI3-kinase activity in wild-type cells by LY294002, exhibit reduced but still very significant chemotaxis (Funamoto *et al.*, 2001). Furthermore, localization of both DdPIK1 and DdPIK2 at the leading edge is independent of PI3-kinase activity, and PTEN localization to the back of the cell is independent of PTEN

This article was published online ahead of print in *MBC in Press* (http://www.molbiolcell.org/cgi/doi/10.1091/mbc.E05–09–0825) on January 18, 2006.

[V] The online version of this article contains supplemental material at *MBC Online* (http://www.molbiolcell.org).

Present addresses: † Department of Biology, National University of Ireland Maynooth, Maynooth, Co. Kildare, Ireland; ‡ Cambridge University, Department of Anatomy, Downing Street, Cambridge CB2 3DY, United Kingdom.

Address correspondence to: Peter J.M. van Haastert (P.J.M.van.Haastert@rug.nl).

activity and PI(3,4,5)P_3 levels (Iijima *et al.*, 2004). These data imply the presence of an underlying mechanism of signal amplification and localization independent of PI(3,4,5)P_3.

To examine the role of PI(3,4,5)P_3 and the underlying PI(3,4,5)P_3-independent mechanism of gradient sensing, we have analyzed several signaling events at a broad range of cAMP-stimulus concentrations and different concentrations of the PI3-kinase inhibitor LY294002. Inhibition of cAMP-stimulated PI(3,4,5)P_3 production by more than 95% has little effect on cAMP-induced cGMP response and the initial phase of actin polymerization, but drastically inhibits the cAMP response and thus autonomous cell aggregation. LY294002-treated cells become very round, which is slowly reversed by cAMP. Round cells show reduced chemotaxis, but once elongated cells exhibit efficient chemotaxis, despite the absence of detectable localization of PHcracGFP at the leading edge. We suggest that severe reduction of PI(3,4,5)P_3 levels has no strong effect on chemotaxis, despite the notion that PI(3,4,5)P_3, when present, is a strong regulator of pseudopod formation.

MATERIALS AND METHODS

Strains and Growth Conditions

The *D. discoideum* strains AX3 (wild type), *dd5p2*-null, and *dd5p1/2*-null (Loovers *et al.*, 2003), were grown in HG5 medium and supplemented with 10 μg/ml G418 when necessary. Two strains with deletion of the two *pi3k1* and *pi3k2* genes were used, the original *ddpik1/2*-null stain (Zhou *et al.*, 1995; friendly gift of R. Firtel) and recreated *pi3k1/2*-null GMP1 cells (Funamoto *et al.*, 2001; obtained from the *Dictyostelium* stock center), yielding similar results. When grown in shaking culture the cell density was kept between 5.10^5 and 6.10^6 cells/ml. LY294002 (dissolved in dimethyl sulfoxide [DMSO]) was added to the cell suspension 15–30 min before cAMP stimulation (maximal 1/400 of total volume); the corresponding amount of DMSO was added to control cells.

Initially, we observed much variation of the concentrations of LY294002 that inhibits several responses. This variation appeared to be due to an instability of LY294002. Using the inhibition by LY294002 of the cAMP-induced cAMP accumulation as assay, we noticed that the LY294002 concentration inducing half-maximal inhibition was 15 μM when stored for 24 h at −80 or 4°C, but 50 μM when LY294002 was stored for ~5 h at room temperature, suggesting 70% degradation at room temperature.

Cell Aggregation, Cell Shape, and Chemotaxis

Cell aggregation and chemotaxis was assayed using nonnutrient hydrophobic agar plates (11 mMKH_2PO_4, 2.8 mM Na_2HPO_4, 7 g/l hydrophobic agar) containing different concentrations of LY294002. To determine aggregation capability, cells were starved in wells under buffer till small aggregation centers of 5–10 cells were formed. Droplets of ~2 μl of 5-h starved cells (6×10^6 cells/ml) were placed on nonnutrient hydrophobic agar plates. The shape of the cells, the aggregation time, and the number of aggregates per droplet were recorded.

Chemotaxis toward cAMP was tested by placing a second droplet, with the indicated concentration of cAMP, next to the droplet of cells, similar to that in the small-droplet chemotaxis assay (Konijn, 1970). Positive chemotaxis is defined as a droplet where twice as many cells are pressed against the side of the higher cAMP concentration as against the other side; reported are the fraction of droplets with a positive response. The shape of the cells and the fraction of droplets with positive chemotactic response were recorded.

Chemotaxis was also tested using micropipettes filled with 10^{-4} M cAMP applied to a field of aggregation competent cells with a Eppendorf femtotip at a pressure of 25 hPa. AX3 cells expressing PHcrac-GFP were observed by confocal fluorescent microscopy to record simultaneously the cellular localization of PHcrac-GFP (see below). AX3 cells and *pi3k1/2*-null cells were also monitored by phase contrast microscopy. The motile behavior of cells in spatial gradients of cAMP was analyzed using computer-assisted methods previously described (Soll, 1999). Briefly, images were recorded every 5 s during a period of 10 min for the confocal microscope and every 30 s during 20 min for the phase-contrast microscope. The contour of the cell and the position of the cell centroid was determined. Chemotactic index, defined as the distance moved in the direction of the pipette divided by the total distance moved, was computed from the centroid positions.

To analyze the shape of the cells, we calculated the roundness of the cell from its contour. An ellipsoid was constructed around the cell as follows (see also below in Figure 6A): First, the ellipsoid and the contour have the same centroid. Second, the ellipsoid will cross the cell contour several times, by which areas a of the cell will be localized outside the ellipsoid, and conversely there will be areas b within the ellipsoid not containing parts of the cell; the ellipsoid was constructed in such a way that $\Sigma a = \Sigma b$. In this way the surface of the ellipsoid equals the surface area of the cell contour. The ellipsoid will have two radii; the roundness is defined as the ratio of short radius divided by long radius. A round ellipsoid approaching a circle will have nearly equal radii, and thus the roundness approaches 1.0. In contrast, an elongated ellipsoid approaching a line will have a short radius close to zero and the roundness approaches 0.0. For the quantitative analysis of cell shape presented in Figure 6, we used a Zigmond chamber consisting starved cells below a 2-mm glass bridge. A linear cAMP gradient is formed from two agar blocks containing cAMP and buffer, respectively, that are placed at opposite sides of the glass bridge.

In Vivo PI(3,4,5)P_3 Production

To determine the amount of PI(3,4,5)P_3, cells were labeled and lipids were extracted essentially as described (Huang *et al.*, 2003). Cells (2.10^7 cells/ml) were starved in MES-DB (20 mM MES, 2 mM $MgSO_4$, and 0.2 mM $CaCl_2$, pH 6.5) and pulsed for 4 h with 100 nM cAMP. Cells were washed once and resuspended in MES-DB at 8.10^7 cells/ml. Radioactive orthophosphate (0.5 mCi ^{32}P per ml cells, 8500–9120 Ci/mmol, NEN Life Sciences Products, Boston, MA) was added and cells were shaken for 40 min. Cells were incubated for another 20 min in the presence of 2.4 mM caffeine, washed three times with MES-DB, and resuspended at 1.10^8 cells/ml. Samples (150 μl) were taken and reactions were stopped with 1 ml of 1 M HCl. After 20–30 min incubation, lipids were extracted using 2 ml MeOH/$CHCl_3$ (1:1) and 2 ml MeOH/H_2O (1:1). Lipids were dissolved in 25 μl MeOH/$CHCl_3$ (1:2), spotted onto TLC plates, and run in $CHCl_3$/acetone/MeOH/acetic acid/water (30:12:10:9:6). Lipids were visualized by exposure to a phosphor imager film and quantified using Image Quant.

PHcrac-GFP Translocation

To determine the cellular localization of PHcrac-GFP, wild-type AX3 cells were transfected with plasmid WF38 (Parent *et al.*, 1998). Cells were stimulated with the indicated concentrations of cAMP using a homemade flow chamber. This chamber allows rapid exchange of solutions without occurrence of gradients; the delay time of the chamber is ~1 s (Potma *et al.*, 2001, 2003). To study the effect of latrunculin A, untreated cells were stimulated with cAMP. Cells were washed with PB and incubated with 1 μM latrunculin A in the chamber. After 20 min these cells were stimulated with cAMP. To study the effect of LY294002, untreated cells were stimulated with cAMP. Cells were washed with PB and treated with increasing amounts of LY294002. After 20 min of treatment with the lowest concentration of LY294002, cells were stimulated with cAMP for 2 min, washed with PB containing the LY294002 concentration necessary for the next stimulation, incubated for 10 min, and stimulated with cAMP. Images were obtained using a Zeiss LSM510 confocal fluorescence microscope (Carl Zeiss, Oberkochen, Germany) with a Plan-Neofluor 40× magnification 1.30 aperture oil immersion objective. The fluorescence intensity in the cytosol was determined as described (Postma *et al.*, 2003) and corrected for the small increase (4%) of circumference of the cell after stimulation.

Actin Polymerization Assay

The amount of F-actin was determined essentially as described (Chen *et al.*, 2003). Cells were starved for 5 h in DB (PB supplemented with 2 mM $MgSO_4$ and 0.2 mM $CaCl_2$) and pulsed with 100 nM cAMP the last 4 h. To achieve a basal level, an equal amount of PM (PB supplemented with 2 mM $MgSO_4$) was added to the suspension and cells were incubated for 15 min with 2 mM caffeine. Cells were collected, resuspended in PM supplemented with 2 mM caffeine at 3.10^7 cells/ml and incubated for another 15 min. At various time points after adding cAMP, samples (100 μl) were taken, fixed, and stained in 1 ml TRITC-phalloidin buffer (3.7% formaldehyde, 0.1% Triton X-100, 250 nM TRITC-phalloidin (Sigma), 20 mM KPO_4, 10 mM PIPES, 5 mM EGTA, 2 mM $MgCl_2$, pH 6.8). Samples were shaken for 1 h, pelleted, resuspended in 1 ml MeOH, and incubated overnight at 200 rpm, and fluorescence was measured (excitation wavelength 544 nm, emission wavelength 574 nm). The same batch of cells was used to measure the effect of LY294002 on the cAMP-stimulated actin polymerization and production of cGMP, and as a control cAMP-stimulated production of cAMP was measured as well.

cGMP and cAMP Assays

In vivo cGMP and cAMP production were measured as described (Snaar-Jagalska and Van Haastert, 1994). In short, cells were starved as described for the actin polymerization assay (cGMP assay) or for 5 h in PB (10 mM Na_2HPO_4/KH_2PO_4, pH 6.5), and resuspended at 1.10^8 cells/ml (cAMP assay). Cells were stimulated with the indicated concentrations of cAMP (cGMP assay) or with 5 μM dcAMP in the presence of 5 mM DTT (cAMP assay). Concentrations of cGMP or cAMP in lysates were determined using the cGMP radioimmunoassay from Amersham or using protein kinase type I from beef muscle, respectively.

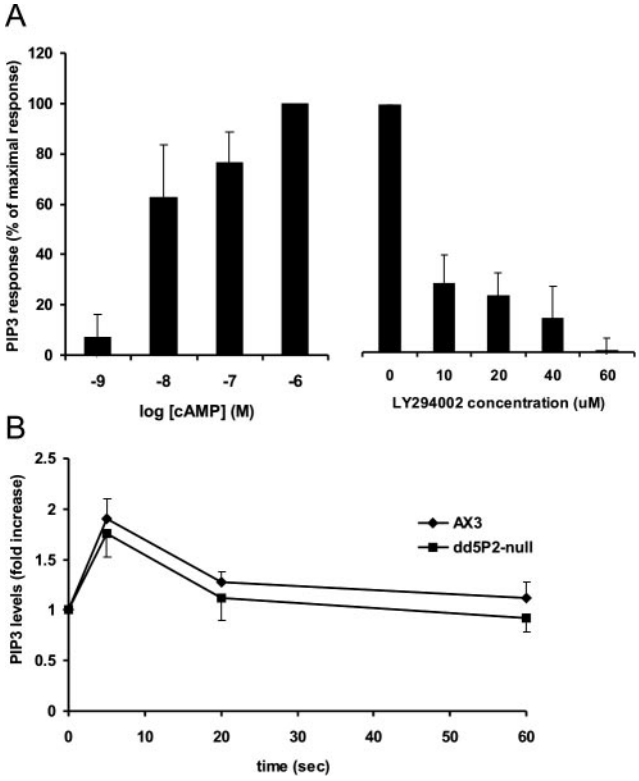

Figure 1. PI(3,4,5)P_3 levels after stimulation with different concentrations of cAMP in the absence and presence of different concentrations of LY294002. Cells were labeled with $^{32}PO_4$, incubated with different concentrations of LY294002 and stimulated with various cAMP concentrations. Reactions were terminated at the indicated times. Phospholipids were isolated, separated by TLC, visualized by exposure to a phosphor imager film, and quantified using Image Quant. Production of PI(3,4,5)P_3 is expressed as the increase of PI(3,4,5)P_3 as percent of the increase observed in cells stimulated with 1 μM cAMP in the absence of inhibitors. In three independent experiments basal and cAMP-stimulated PI(3,4,5)P_3 levels in arbitrary units are 3711 and 6375, 9967 and 16505, and 10700 and 22000, respectively. (A) Left panel, AX3 cells were stimulated with the indicated cAMP concentrations. Samples were taken before stimulation and 5 s after stimulation. Right panel, cells were incubated for 15 min with the indicated LY294002 concentrations and stimulated with 1 μM cAMP. Samples were taken before and 5 s after stimulation. (B) Time course of PI(3,4,5)P_3 production of AX3 and *dd5p2*-null cells stimulated with 1 μM cAMP.

RESULTS

Stimulation of *D. discoideum* with the chemoattractant cAMP leads to a transient increase of PI(3,4,5)P_3 levels (Huang *et al.*, 2003). The levels of other signaling molecules, including cAMP and cGMP, as well as F-actin, are also transiently elevated. To elucidate the role of PI(3,4,5)P_3 in chemotaxis we investigated the effect of reduced PI3-kinase activity using the PI3-kinase inhibitor LY294002.

Dependence of PI(3,4,5)P_3 Production on the Activity of PI3-Kinases and Inositol 5-phosphatases

We measured the change in PI(3,4,5)P_3 levels upon stimulation with cAMP in vivo, using cells labeled with ^{32}P orthophosphate and separation of lipids by TLC. A significant amount of PI(3,4,5)P_3 was produced when cells were stimulated with 1 μM cAMP in the absence of PI3-kinase inhibitors (Figure 1). Stimulation with 1 nM cAMP resulted in a small PI(3,4,5)P_3 accumulation, whereas at 10 nM cAMP the amount of PI(3,4,5)P_3 produced was ~60% of the amount with 1 μM cAMP (Figure 1A). Half-maximal accumulation of PI(3,4,5)P_3 levels is estimated to be induced by 5 nM cAMP.

The amount of PI(3,4,5)P_3 accumulation is determined by the combined action of enzymes that produce and degrade PI(3,4,5)P_3. We investigated the PI(3,4,5)P_3 response in cells with modified activities of these enzymes. The most important PI(3,4,5)P_3 producing enzymes in *D. discoideum* are the PI3-kinases that phosphorylate PI(4,5)P_2 at the 3-position. When cells were treated with 60 μM PI3-kinase inhibitor LY294002, the in vivo production of PI(3,4,5)P_3 induced by 1 μM cAMP was inhibited by 95%. The response was already substantially inhibited up to 75% at 10 μM LY294002; therefore we estimate half-maximal inhibition in vivo to occur at 6 μM LY294002 (Figure 1B). These results show that LY294002 acts as a potent PI3-kinase inhibitor in vivo, confirming previous reports that LY294002 inhibits PI(3,4,5)P_3 production in vitro; however, half-maximal inhibition in vitro was observed at ~20 μM LY294002 (Huang *et al.*, 2003).

PI(3,4,5)P_3 can be degraded by inositol 3-phosphatases and multiple inositol 5-phosphatases (Funamoto *et al.*, 2002; Iijima and Devreotes, 2002; Loovers *et al.*, 2003). Inactivation of the 3-phosphatase PTEN results in a strong and prolonged PI(3,4,5)P_3 response (Huang *et al.*, 2003). PI(3,4,5)P_3 is also degraded by *D. discoideum* inositol 5-phosphatases in vitro, notably by Dd5P2. We measured PI(3,4,5)P_3 levels in *dd5p2*-null cells, which exhibit enhanced chemotaxis toward cAMP (Loovers *et al.*, 2003). However, when stimulated with 1 μM cAMP no significant difference was observed in the in vivo PI(3,4,5)P_3 production compared with wild-type AX3 cells (Figure 1C).

Effect of LY294002 and Latrunculin A on PHcrac-GFP Localization

PI(3,4,5)P_3 is one of the key second messengers for targeting proteins transiently to the membrane. One of these proteins is CRAC is a cytosolic regulator of adenylyl cyclase A. The PH domain of CRAC, fused to GFP (PHcrac-GFP), is often used as an indicator for PI(3,4,5)P_3 production (e.g., Parent *et al.*, 1998; Funamoto *et al.*, 2002; Postma *et al.*, 2003; Dormann *et al.*, 2004). Uniform stimulation with 1 μM cAMP results in a nearly uniform translocation of PHcrac-GFP to the membrane and is frequently followed by a second patchlike response (Figure 2A). The appearance of the second response in PHcrac-GFP translocation shows a strong dependency on the condition of the cells (unpublished observations). Analysis of the fluorescence intensity of PHcrac-GFP in the cytosol revealed that the first response was inhibited half-maximal at ~10 μM LY294002 (Figure 2B). Although at 50 μM LY294002 no cAMP-stimulated increase of fluorescence intensity at the membrane could be observed by eye (Figure 2A), the very accurate analysis of the fluorescence intensity in the cytosol showed that a residual response of ~10–15% is still present at concentrations as high as 60 μM LY294002 (Figure 2B). Similar observations have been made using another detector of PI(3,4,5)P_3, showing that LY294002 inhibits translocation of this PH-domain to the membrane with half-maximal effect at 10–30 μM, leaving a small residual translocation of ~15–20% at saturating doses of LY294002 (Funamoto *et al.*, 2001). As mentioned, PHcrac-GFP translocation shows a biphasic response. The data on the fluorescence intensity of the cytosol showed that the second patchlike response is also inhibited by LY294002 with half-maximal effect at ~20 μM; as with the first response, inhibition of the second response at 60 μM

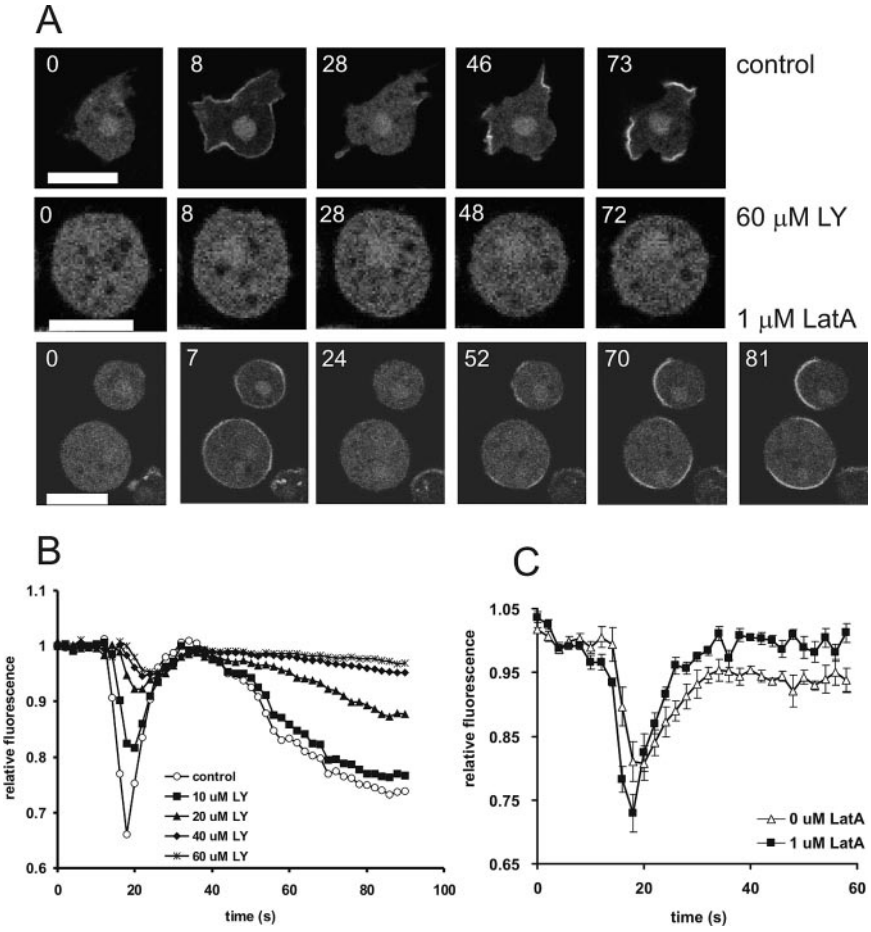

Figure 2. Effect of LY294002 and latrunculin A on PHcrac-GFP translocation. Cells were uniformly stimulated with 1 μM cAMP. Confocal images were obtained and translocation of PHcrac-GFP was determined by measuring the fluorescence intensity of PHcrac-GFP in the cytosol. (A) Translocation of PHcrac-GFP in untreated cells (control), in cells treated for 15 min with 60 μM LY294002 (LY), or in cells treated for 5 min with 1 μM latrunculin A (LatA). The figures show a typical cell at different times (s) after stimulation with 1 μM cAMP; bars, 10 μm; see Supplementary Movie. (B) Normalized fluorescence intensity of PHcrac-GFP in the cytosol in cells treated with different concentrations of LY294002 after stimulation with 1 μM cAMP. Left panel, time course with cAMP addition at t = 10 s. (C) Normalized depletion of PHcrac-GFP in the cytosol in untreated cells and cells treated with 1 μM latrunculin A after stimulation with 1 nM cAMP at t = 10 s.

LY294002 was not complete. In cells starved for shorter periods, the second patchlike translocation often occurs to macropinosomes instead of pseudopodia. We noticed that inhibition of PHcrac-GFP translocation to macropinosomes requires ~twofold higher LY294002 concentrations than inhibition of translocation to pseudopodia (unpublished data).

In neutrophils evidence exists that F-actin enhances the accumulation of $PI(3,4,5)P_3$, thereby providing a positive feedback mechanism (Wang *et al.,* 2002; Weiner *et al.,* 2002; Li *et al.,* 2003; Xu *et al.,* 2003). A similar mechanism has been proposed to exist in *D. discoideum* (Sasaki *et al.,* 2004), but has not been strongly supported (Parent and Devreotes, 1999; Janetopoulos *et al.,* 2004; Postma *et al.,* 2004). When cells are treated with the F-actin inhibitor latrunculin A and placed in a gradient, a PHcrac-GFP patch is present at the front of the cells (Parent *et al.,* 1998). To explore the role of F-actin on the localized accumulation of $PI(3,4,5)P_3$, we incubated *Dictyostelium* cells with 1 μM of latrunculin A, followed by stimulation with different cAMP concentrations. Uniform stimulation with 1 μM cAMP induces a normal translocation of PHcrac-GFP to the membrane (Postma *et al.,* 2003; Figure 2A); the initial PHcrac-GFP patches are essentially identical in control and latrunculin A-treated cells with respect to fluorescence intensity, size, and number of patches. In cAMP-stimulated control cells a pseudopod is extended from an area with a PHcrac-GFP patch. After ~1 min the PHcrac-GFP patch and pseudopod disappear and a new PHcrac-GFP patch and pseudopod is formed at another area of the cell. In latrunculin A-treated cells, pseudopodia are not extended and PHcrac-GFP patches do not have a limited lifetime. Instead of disappearing, the area of the PHcrac-GFP patch broadens, and often patches fuse (see Figure 2A, and Supplementary Movie 3). The final state at ~2–3 min after stimulation is a cell with either a single patch or a cell with two patches at opposite sites of the cell; these PHcrac-GFP patches have the same fluorescence intensity as patches in control cells, but are larger and have less sharp boundaries. To determine if latrunculin A affects PHcrac-GFP localization at low cAMP concentrations, we measured depletion of PHcrac-GFP in the cytosol at 1 nM cAMP. However, we could not observe any difference in the initial PHcrac-GFP translocation after latrunculin A treatment compared with control cells (Figure 2C). We conclude that inhibition of F-actin and pseudopod formation does not affect the local formation of $PI(3,4,5)P_3$, but affects the boundary of these patches such that they become less confined.

Effect of LY294002 on cAMP-induced Actin Polymerization

Uniform stimulation of *D. discoideum* with cAMP results in a temporary increased actin polymerization, which peaks around 5 s after stimulation, sometimes followed by a second actin polymerization response around 120 s after stimulation. PHcrac-GFP and F-actin colocalize during the first uniform response at the membrane and during the second response in random pseudopodia. They also colocalize at the leading edge in a cAMP gradient (Funamoto *et al.,* 2002; Iijima and Devreotes, 2002; Chen *et al.,* 2003). Previous reports in *D. discoideum* show that LY294002 does not effect the

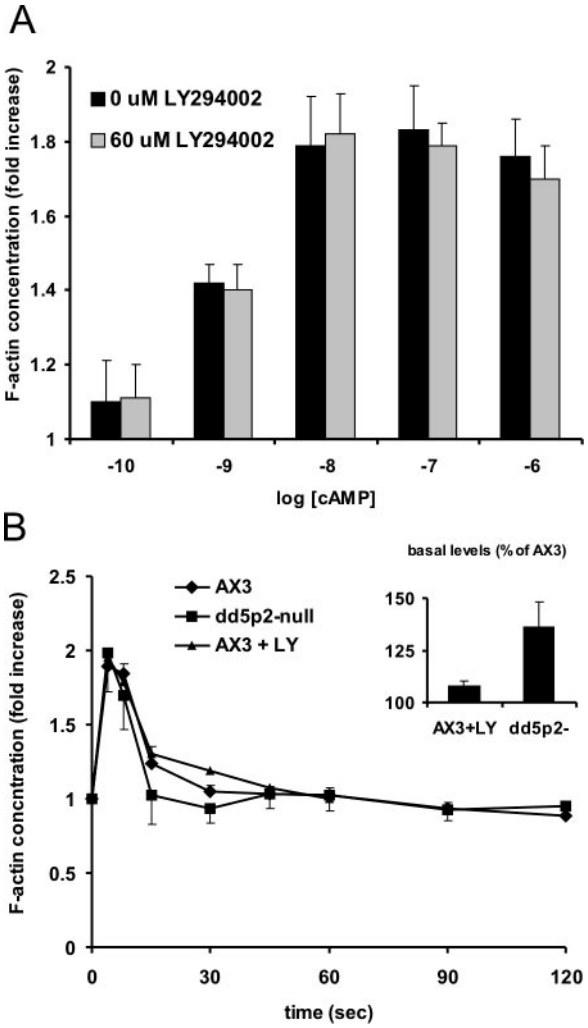

Figure 3. Effect of PI3-kinase inhibition and inositol 5-phosphatase inactivation on actin polymerization. (A) Cells were incubated with or without 60 μM LY294002 and stimulated with different cAMP concentrations. Samples were taken 4 s after stimulation. The amount of F-actin is expressed as the fold increase compared with basal levels. (B) Time course of wild-type (AX3) and *dd5p2*-null cells. Cells were stimulated with 1 μM cAMP and samples were taken at the indicated time points. Insert, basal levels of F-actin in *dd5p2*-null and AX3 cells with LY294002.

first actin polymerization response when cells are stimulated with 1 μM cAMP but that it completely eliminated the second response (Chen *et al.*, 2003). We investigated whether we could observe an effect at lower cAMP concentrations. Therefore, we measured the F-actin response induced by 0.1 nM to 1 mM cAMP in vivo in the absence or presence of 60 μM LY294002, which maximally inhibits PI(3,4,5)P_3 production. The cAMP-stimulated F-actin production of LY294002-treated cells exhibited similar magnitude (Figure 3A) and kinetics (Figure 3B) compared with the response of control cells; basal F-actin levels are also not affected by LY294002. In addition, inactivation of the inositol 5-phosphatase Dd5P2 did not alter the kinetics of actin polymerization, although basal levels were slightly increased (Figure 3B). In the current experiments we did not reliably observed a second actin polymerization response in control or mutant cells, so we cannot assess the effect of LY294002 on it.

Effect of LY294002 on cGMP and cAMP Production

The second messengers cAMP and cGMP are produced upon stimulation of *D. discoideum* with cAMP. The combined action of guanylyl cyclases and phosphodiesterases leads to a transient increase in cGMP that reaches its maximum 10 s after stimulation (reviewed in Bosgraaf and Van Haastert, 2002). We measured this in vivo response at different concentrations of cAMP and LY294002. Inhibition of PI3-kinases by LY294002 did not lead to any changes in cGMP production at both micromolar and nanomolar concentrations of chemoattractant (Figure 4A). Also for the *ddpik1/2*-null cell line no significant differences were observed (Figure 4B).

Extracellular cAMP also activates adenylyl cyclase ACA. The produced intracellular cAMP is secreted and activates nearby cells thereby relaying the chemotactic signal (reviewed in Saran *et al.*, 2002). We measured the total amount of cAMP production, inhibiting phosphodiesterase activity with DTT. In stimulated control cells cAMP production increases strongly during the first few minutes and then levels off due to adaptation (Figure 5A). Wild-type cells treated with 60 μM LY294002 exhibit a smaller cAMP accumulation that is ~25–30% of control cells. The cAMP accumulation of *pi3k1/2*-null cells is also strongly reduced to ~25% of the response of wild-type cells (Figure 5A); we obtained similar results in another PI3K-null strain, *ddpik1/2*$^-$ (Zhou *et al.*, 1998; unpublished data). This residual cAMP response of *pi3k1/2*-null cells is completely inhibited by 60 μM LY294002 (Figure 5A). The cAMP accumulation at different concentrations of LY294002 reveal that the response of wild-type cells is inhibited by relatively low concentrations with half-maximal inhibition at ~5 μM and maximal inhibition at 10 μM LY294002 (Figure 5B). Increasing the LY294002 concentration up to 60 μM did not further reduce cAMP production. In *pi3k1/2*-null cells, slightly higher concentrations of LY294002 are required to obtain inhibition, with half-maximal effect at ~10 μM and complete inhibition at 20 μM LY294002. The results demonstrate that inhibition of PI3K activity by LY294002 in wild-type cells or deletion of two PI3K encoding genes in *ddpik1/2*-null cells lead to partial 70–80% inhibition of cAMP relay. This partial response in *ddpik1/2*-null cells can be inhibited completely by LY294002, suggesting that the residual response is mediated by other PI3-kinases that are inhibited by LY294002.

In wild-type cells, the cAMP accumulation reaches a plateau at ~2–3 min after stimulation, which is caused by adaptation of the cells to the constant stimulus concentration. The results of Figure 5A suggest that in *pi3k1/2*-null cells cAMP levels continue to increase for longer periods of time. This late cAMP response may indicate that PI3K signaling is required for both activation and adaptation of ACA as suggested recently by Comer and Parent (2006). If PI3K signaling is required for adaptation, we would expect that the late cAMP response increases in the presence of LY294002. However, we observed the opposite, with complete inhibition of the late cAMP accumulation at very low concentrations of LY294002. For instance, treatment of *pi3k1/2*-null cells with 5 μM LY294002 has little effect on the early cAMP accumulation, but the late response is strongly inhibited (Figure 5A). In conclusion, the cAMP response is inhibited partly in wild type by LY294002 or in *pi3k1/2*-null cells and completely by LY294002 in *pi3k1/2*-null cells. Furthermore, the kinetics of the response may be altered by inhibition of PI3K activity because of differential effects on activation and adaptation of the response.

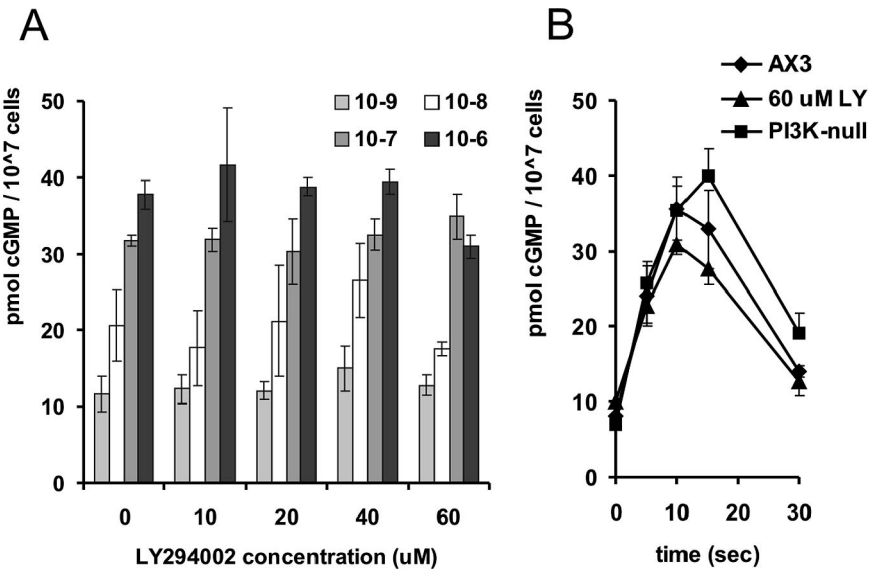

Figure 4. Effect of PI3-kinase inhibition on cGMP production. (A) Production of cGMP was measured in wild-type cells treated with the indicated amounts of LY294002 after stimulation with different cAMP concentrations. cGMP concentrations were determined before stimulation and 10 s after stimulation. (B) Time course of wild-type cells (AX3), *ddpik1/2*-null cells and AX3 cells treated with 60 μM LY294002. Cells were stimulated with 1 μM cAMP and samples were taken at the indicated time points.

Effect of LY294002 on Cell Shape

Addition of LY294002 has been shown to induce the rounding of elongated cells (Funamoto *et al.,* 2001, 2003; Iijima and Devreotes, 2002; Chen *et al.,* 2003). The contour of a cell can be approximated by an ellipsoid, which has a long and a short axis (see Figure 6A and *Materials and Methods*). We determined the roundness of the cell by calculating the ratios of the long and the short axis of the ellipsoid. A circle has equal axis and a roundness of 1.0, whereas a very elongated cell will approach a line segment with a roundness of 0.0. Aggregation competent cells in buffer have a roundness of 0.39 $\pm$ 0.17. Addition of 60 μM LY294002 induces a strong rounding of the cell to 0.84 $\pm$ 0.12, with half-maximal effect at 20 μM LY294002 (Figure 6B). Interestingly, addition of cAMP to these LY294002-treated cells induces a recovery of the elongated shape in a time dependent (Figure 6C and E) and cAMP-dose dependent manner (Figure 6D). Addition of 500 nM cAMP to control cells induces a small reduction of the roundness from 0.39 $\pm$ 0.17 to 0.30 $\pm$ 0.08. The roundness of LY294002-treated cells start to decrease at ~1 min after addition of 500 nM cAMP, and approaches the roundness of control cAMP-treated cells after ~10 min; half-maximal recovery of the elongated shape was obtained at ~2–3 min after addition of cAMP (Figure 6E). Low concentrations of cAMP up to ~5 nM have little effect on the roundness of LY294002-treated cells. Maximal recovery was observed at ~500 nM cAMP with half-maximal effect at ~15 nM cAMP (Figure 6D).

Effect of LY294002 on Cell Aggregation

Cell aggregation requires the production and secretion of cAMP, as well as cell movement and chemotaxis toward the source of cAMP. We starved cells in wells under buffer till small aggregation centers of 5–10 cells were formed. Then cells were resuspended and transferred as small droplets on hydrophobic agar containing different concentrations of LY294002. In the absence of LY294002, aggregation centers start to form 25 min after placing droplets of starved cells on hydrophobic agar. The presence of LY294002 at 20 μM or higher concentrations caused the cells to round up temporary and aggregation was inhibited (Table 1). The delay in aggregation was only a few minutes at 20 μM LY294002, but increased strongly to 2–3 h at 60 μM LY294002 (Table 1). Cell aggregation started at about the same time that the round cells adopted an elongated shape. Although eventually all cells are incorporated into cell aggregates, the number of aggregates per droplet increases at higher concentrations of LY294002. This effect is consistent with the inhibition of cAMP relay by LY294002, which will lead to a reduction of autonomous cAMP signaling.

Effect of LY294002 on Chemotaxis

The previous results demonstrate that inhibition of PI3-kinase by LY294002 induces the cells to round-up and that cAMP concentration above 100 nM can restore this effect. To investigate the effect of LY294002-treatment on chemotaxis, we determined the chemotaxis index while cells were still round or when cells had recovered to an elongated shape.

Cells placed on agar containing different concentrations of LY294002 were subjected to a spatial gradient of cAMP by placing a droplet of 1 μM cAMP next to the droplet of cells. At 20 μM LY294002, cells close to the droplet of cAMP were polar with extending pseudopodia after 20 min of applying the cAMP droplet, whereas cells further away from the cAMP were still round (Figure 7). After 45 min, essentially all cells were elongated and made protrusions at the front, even on agar with the highest concentration of 60 μM LY294002 (unpublished data). Chemotaxis to cAMP on agar is measured as the percentage of cell populations responding to the cAMP gradient. The results presented in Table 2 show that cAMP concentrations that do restore cell shape of LY294002-treated cells (100 and 1000 nM cAMP) also induce a chemotactic response that is indistinguishable from the chemotactic response of control cells, whereas cAMP concentrations that do not restore cell shape (1 or 10 nM cAMP) will induce a chemotactic response in control cells but not in LY294002-treated cells.

We have also used a micropipette assay for chemotaxis as used by others and determined the chemotaxis index and speed by computer-assisted analysis of the cell tracks. Using a pipette filled with 10^{-4} M cAMP, the majority of control cells exhibit strong localization of PHcrac-GFP at the leading edge (Figure 8A) and have a chemotaxis index of 0.81 $\pm$ 0.05 (Table 2). As in previous experiments, cells incubated with 60 μM LY294002 are round. During the first minute after application of the gradient, these LY294002-treated cells stay

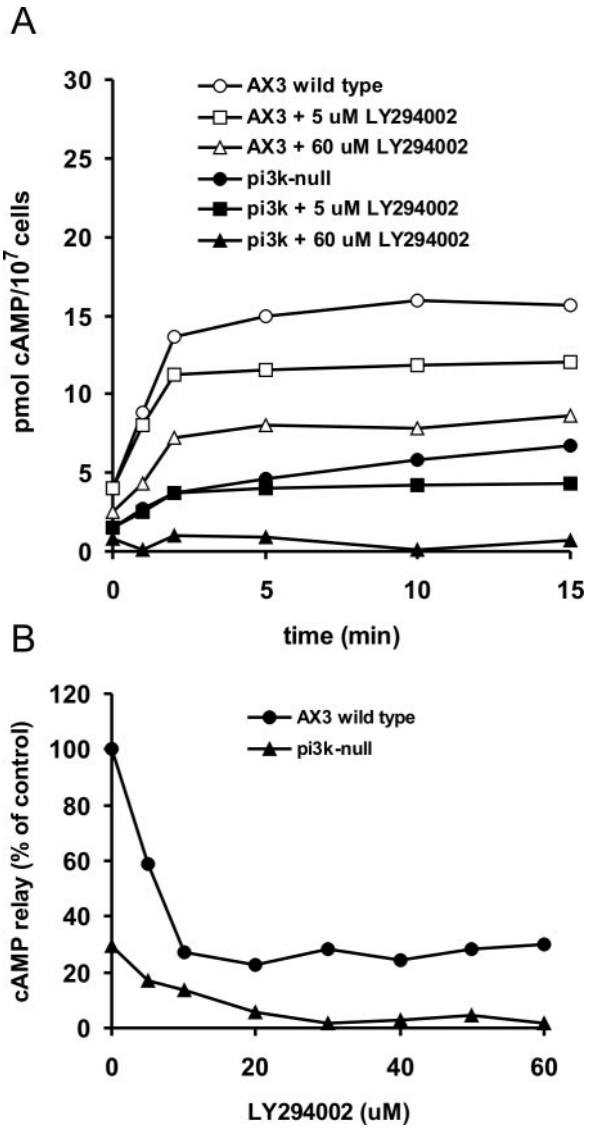

Figure 5. Effect of PI3-kinase inhibition on cAMP production. Cells were preincubated with the indicated concentration of LY294002 for 15 min, followed by stimulation with 5 μM 2′deoxy-cAMP in the presence of the phosphodiesterase inhibitor dithiothreitol, and cAMP levels were measured at the indicated time points. (A) Time course of wild-type AX3 and *pi3k1/2*-null cells in the presence and absence of 5 or 60 μM LY294002. (B) Dose-response curves. AX3 and pi3k1/2-null cells were incubated with different concentrations of LY294002 and samples were taken at 0, 2, 5, and 10 min after stimulation with 5 μM 2′deoxy-cAMP and dithiothreitol. The data are presented as the increase of cAMP levels (from 0 min to the mean of 2, 5, and 10 min) as % of the increase in wild-type cells in the absence of LY294002.

rather round, have poor chemotaxis, and do not show localization of PHcrac-GFP at the membrane (unpublished data). The cells become polarized 2–3 min after the cAMP gradient was delivered from the pipette. These cells still do not exhibit localization of PHcrac-GFP at the leading edge (Figure 8B), but show rather efficient chemotaxis with a chemotaxis index of 0.75 ± 0.13, which is not significantly different from the chemotaxis index of control cells (Table 2). We also measured the speed of the same cells for the same time period as reported on chemotaxis index. In contrast to chemotaxis index, the speed of the cells is significantly reduced by 60 μM LY294002 from 12.41 ± 1.75 μm/min of control cells to 9.21 ± 0.26 μm/min in cells treated with 60 μM LY294002.

Finally, we assayed *pi3k1/2*-null cells for chemotaxis in the absence and presence of LY294002. The chemotaxis index of *pi3k1/2*-null cells is rather high, 0.80 ± 0.13, comparable to that of wild-type cells (Table 2, see also Supplementary Movie 2); in addition, the speed of *pi3k1/2*-null cells is not very different from that of wild-type cells. On addition of 60 μM LY294002, cells become round and immobile, but after positioning of a pipette filled with 10^{-4} M cAMP the majority of the *pi3k1/2*-null cells become elongated and move toward the pipette (see Supplementary Movie 1). The chemotaxis index of these elongated LY294002-treated *pi3k1/2*-null cells is also very high, 0.78 ± 0.08, not significantly different from the chemotaxis index of untreated *pi3k1/2*-null cells (Table 2). As in wild-type cells, LY294002 induced a dramatic reduction of the speed of locomotion from 11.58 ± 1.28 to 5.10 ± 1.26 μm/min.

DISCUSSION

We have shown that cAMP-mediated responses in *D. discoideum* have different dependencies on LY294002 (summarized in Figure 9). PHcrac-GFP translocation is induced by low cAMP concentrations with half-maximal effect at 0.5 nM cAMP (Postma *et al.*, 2003). In contrast, PI(3,4,5)P_3 formation requires higher cAMP concentrations with half-maximal effect at ~5 nM cAMP (this report). These data suggest that relatively low PI3-kinase activity, resulting in a small increase in PI(3,4,5)P_3 levels, is sufficient for maximal PHcrac-GFP translocation. The observation that inhibition of PHcrac-GFP translocation requires higher concentrations of LY294002 than inhibition of PI(3,4,5)P_3 formation also suggests that PHcrac-GFP translocation occurs at subsaturating PI(3,4,5)P_3 levels. Treatment of cells with 60 μM LY294002 completely inhibits the cAMP-stimulated PI(3,4,5)P_3 accumulation, but cells still show a small but significant (~15%) depletion of cytosolic PHcrac-GFP (this report) and PhdA-GFP (Funamoto *et al.*, 2001). This suggests that LY294002 does not inhibit all PI3-kinase activity and that the hypothetical small increase of PI(3,4,5)P_3, which we cannot detect, is sufficient to mediate 15% translocation of PHcracGFP upon uniform cAMP stimulation.

The 3-phosphatase PTEN and multiple 5-phosphatases, especially Dd5P2, have been reported to degrade PI(3,4,5)P_3 in vitro. Inactivation of the inositol 5-phosphatases results in minor phenotypic changes with respect to chemotaxis, whereas *pten*-null cells do show severe defects (Funamoto *et al.*, 2002; Iijima and Devreotes, 2002; Loovers *et al.*, 2003). To investigate the relative contributions of 3-phosphatase and 5-phospatase in the degradation of PI(3,4,5)P_3, we compared the accumulation and decline of cAMP-stimulated PI(3,4,5)P_3 levels in *pten* and *dd5p2* null cells. The difference in PI(3,4,5)P_3 accumulation of *dd5p2* null cells and wild-type cells is within the error of the assay and therefore Dd5P2 contributes to <10% of total phosphatase activity. In wild-type cells ~75% of PI(3,4,5)P_3 is degraded in 15 s, whereas in *pten*-null cells only 15% is degraded within 15 s (Huang *et al.*, 2003). If PI(3,4,5)P_3 degradation in *pten* null cells is only performed by inositol 5-phosphatases, then it is calculated that in wild-type cells roughly 83% is degraded at the 3-position by PTEN and 17% by the sum of 5-phosphatase activities. Using the PH domain of TAPP1, which specifically detects PI(3,4)P_2, Dormann *et al.* (2004) demonstrated the transient accumulation of PI(3,4)P_2 in phagocytic cups, but

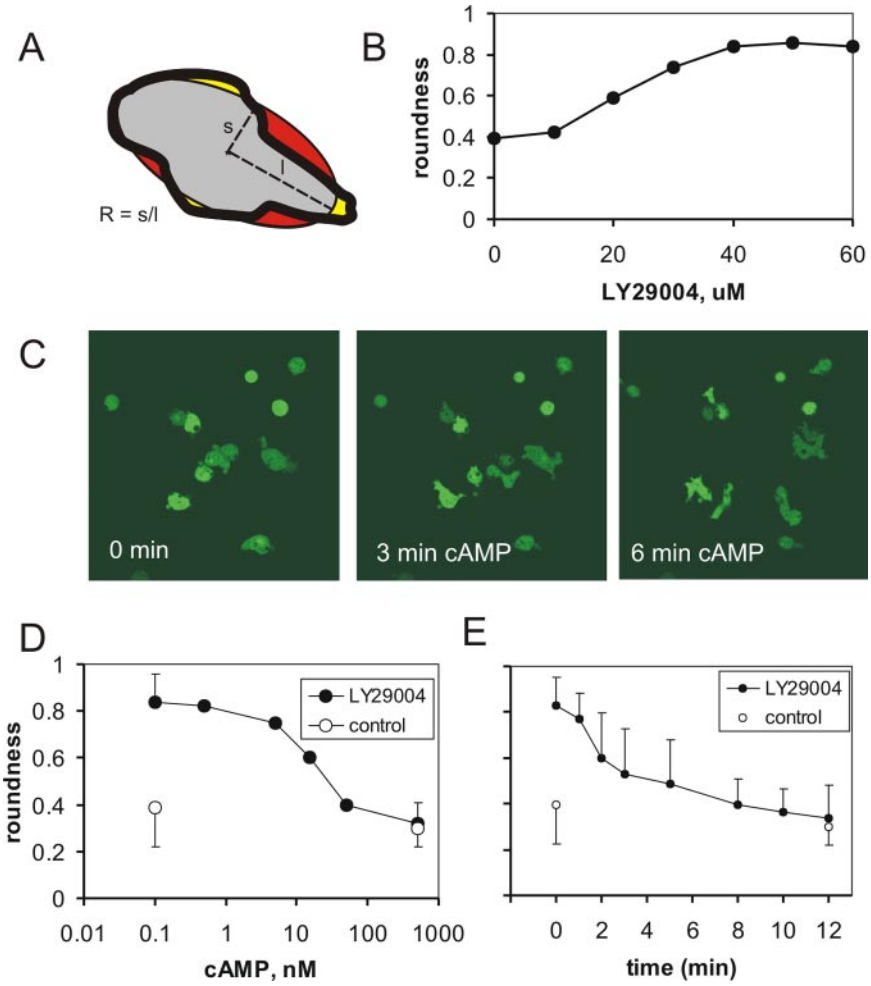

Figure 6. Effect of LY294002 and cAMP on cell shape. (A) Roundness was calculated (see *Materials and Methods*) by calculating the centroid (asterisk) and contour (thick line) of a cell. The ellipsoid (thin line) has the same centroid, and crosses the cell contour several times isolating segments inside the cell but outside the ellipsoid (yellow) or segments inside the ellipsoid but outside the cell (red). The ellipsoid was optimized such that sum of the red surface areas equals that of the yellow areas. Roundness is defined as the ratio of the short and long axis of the ellipsoid. (B) Cells were incubated with different concentrations of LY294002 and the roundness was determined after 15 min. (C) Cells incubated with 60 μM LY294002 for 15 min were stimulated with 1 μM cAMP and confocal images were taken at 0, 3, and 6 min after cAMP addition. (D) Cells were incubated with 60 μM LY294002 for 15 min followed by cAMP at the indicated concentrations. Roundness was determined at 10 min after cAMP addition. (E) Cells were incubated with 60 μM LY294002 for 15 min followed by 500 nM cAMP. Roundness was determined at different times after cAMP addition.

not during chemotactic stimulation by cAMP. Thus the small amount of PI(3,4,5)P_3 degraded by 5-phosphatases does not lead to the accumulation of PI(3,4)P_2, probably because it is readily degraded.

The Function of PI(3,4,5)P_3 in Cell Aggregation

Extracellular stimulation of *Dictyostelium* cells leads to the activation of adenylyl cyclase ACA, which depends on CRAC and translocation of CRAC to the membrane. The production of cAMP is essential for cell aggregation and completely absent in *crac*-null cells (Parent *et al.*, 1998). Consequently, inactivation of either *aca* or *crac* prevents cells to form aggregates and to enter the developmental cycle (Pitt *et al.*, 1992; Insall *et al.*, 1994). We show that either inhibition of PI3-kinase activity by LY294002 or inactivation of two PI3-kinase encoding genes strongly, but not completely, inhibits cAMP production after cAMP stimulation. At concentrations above 20 μM LY294002, ~25% of maximal cAMP production remains, most likely caused by the incomplete inhibition of the translocation of CRAC to the membrane as shown above. A similar small cAMP response was observed in *pi3k1/2*-null cells, in contrast to other reports (Zhou *et al.*, 1998;Comer and Parent, 2006). In *pi3k1/2*-null cells two of the six potential genes encoding PI3-kinases have been disrupted. These cells do not exhibit a detectable PI(3,4,5)P_3 response and translocation of CRAC to the membrane upon cAMP stimulation (Huang *et al.*, 2003). Basal PI(3,4,5)P_3 levels become detectable in p*i3k1/2*-null cells upon deletion of the PI(3,4,5)P_3-degrading enzyme PTEN, indicating that p*i3k1/2*-null cells do make PI(3,4,5)P_3 (Janetopoulos *et al.*, 2005). Interestingly, the small cAMP response in *pi3k1/2*-null cells was completely inhibited by LY294002, suggesting that other PI3-kinases were responsible for residual PI(3,4,5)P_3 production and ACA activation.

Table 1. Effect of LY294002 on aggregation and cell polarity

LY294002 (μM)	Time of aggregation (min)	Period of round cells (min)	Aggregates per droplet
0	25	0	2.77 ± 1.21
10	30	0	3.07 ± 1.54
20	50	10–45	4.76 ± 1.92
40	115	10–110	5.21 ± 2.11
60	145	10–150	5.17 ± 1.39

Droplets of 5-h-starved AX3 cells were deposited onto nonnutrient agar plates containing the indicated concentrations of LY294002. The time of cell aggregation (30% of cells incorporated in cell aggregates and the shape of the cells (round cells have roundness above 0.55) were recorded at different times after deposition of the cells (means of three experiments). The number of aggregates per droplet was determined when more then 90% of the cells were incorporated in aggregates (mean ± SD; n = 26).

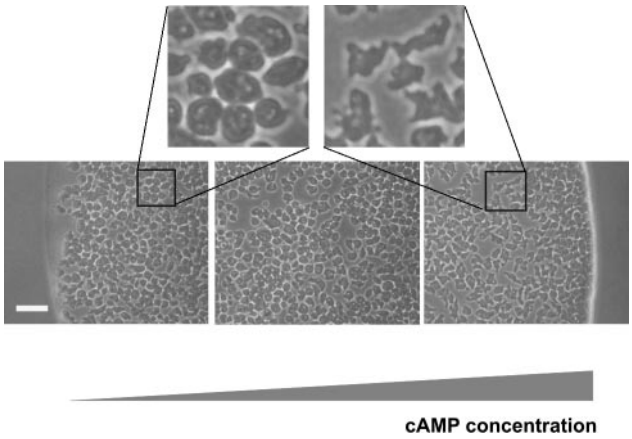

Figure 7. Morphology and chemotaxis of LY294002 treated cells after exposure to a cAMP gradient. Droplets of 5-h starved wild-type AX3 cells were deposited on nonnutrient agar plates containing 60 μM LY294002. Droplets containing 1 μM cAMP were deposited at the right-hand side of the cell droplets. The droplets containing cells or cAMP have a diameter of ~400 μm, and the centers are ~600 μm apart. Shown are segment of a droplet at 20 min after deposition of cAMP; bar, 20 μm. The right panel shows that cells close to the cAMP droplet are elongated and have moved in the direction of cAMP, whereas cells far away from the cAMP droplet (left panel) are still round and have not moved. Data on roundness and chemotaxis at other concentrations of LY294002 and cAMP are presented in Table 2.

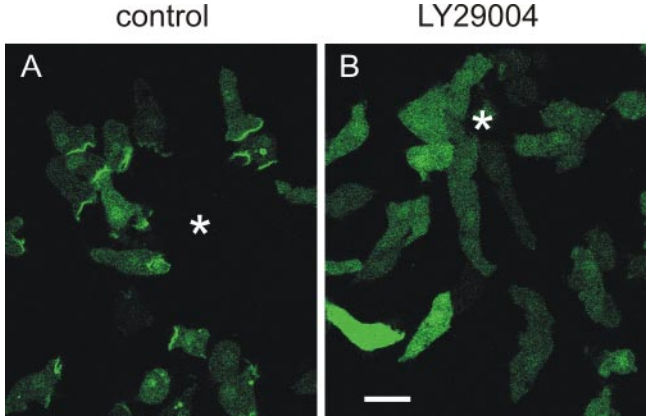

Figure 8. Morphology and localization of PHcrac-GFP in LY294002 treated cells after exposure to a cAMP gradient. PHcrac-GFP-labeled cells were incubated with 60 μM LY294002 for 15 min and then stimulated with a micropipette containing 100 μM cAMP. The confocal images were recorded at 1 min (A) and 5 min (B) after placing the pipette at the position of the asterisk; bar, 10 μm. See Table 2 for chemotaxis data.

The cAMP accumulation of *pi3k1/2*-null cells is reduced compared with wild-type cells, but continues for longer periods. This could mean that PI3K signaling is required for both activation of ACA (explaining reduced cAMP accumulation) and adaptation (explaining prolonged cAMP accumulation), consistent with a detailed study on the role of PI3K signaling on the activation and adaptation of ACA (Comer and Parent, 2006). However, inhibition of PI3K signaling with LY294002 does not lead to prolonged cAMP accumulation in wild-type cells, and it inhibits the prolonged accumulation in *pi3k1/2*-null cells. Many experiments indicate that ACA is regulated by complex pathways. These pathways not only consists of activation and adaptation, but also multiple signaling components besides CRAC translocation to the membrane, including heterotrimeric G-proteins, small G-proteins of the Ras family, RasGEFreceptor,

Table 2. Effect of LY294002 on chemotaxis

	Small population assay				Pipette assay			
	Chemotaxis (%)				Chemotaxis (CI)		Speed (μm/min)	
	Wild-type cells				Wild-type	*pi3k1/2*$^-$	Wild-type	*pi3k1/2*$^-$
LY294002 (μM)	1 Nm cAMP[a]	10 nM cAMP[a]	100 nM cAMP[a]	1000 nM cAMP[a]	100 μM cAMP[b]	100 μM cAMP[b]	100 μM cAMP[b]	100 μM cAMP[b]
0	30	60	90	100	0.81 ± 0.05	0.80 ± 0.13	12.41 ± 1.75	11.58 ± 1.28
10	30	60	90	100	ND	ND	ND	ND
20	9	25	95	100	ND	ND	ND	ND
40	0	0	85	100	ND	ND	ND	ND
60	0	0	87	100	0.75 ± 0.13	0.78 ± 0.08	9.21 ± 0.26	5.10 ± 1.26

Small population assay: Droplets of starved AX3 cells were deposited onto nonnutrient agar plates containing the indicated concentrations of LY294002. A droplet of the indicated cAMP concentration was placed next to the droplet of cells, and the percentage of the populations that showed positive chemotaxis was determined. The data are the means of two experiments with 20 droplets for each condition. The cAMP concentration at the cell is about two- to fivefold lower than the applied cAMP concentration (Mato *et al.*, 1975). Pipette assay: A droplet of 5-h-starved wild-type AX3 cells or *pi3k1/2*-null cells was deposited onto a glass surface in the absence or presence of 60 μM LY294002. A pipette with 100 μM cAMP was placed in the droplet just above the glass surface, and the cells were observed by microscopy during 15 min. The chemotaxis index and speed of cells from 50 to about 200 μm from the pipette were determined for control cells during the entire period and for LY294002-treated cells when they adopted an elongated shape (roundness below 0.5; from 6 to 15 min). The cAMP concentration in the pipette is 100 μM, resulting in a cAMP concentration around the cells of 200–50 nM (at 50 and 200 μm from tip, respectively); data are the means ± SDs from two experiments with each 24–26 cells. Supplementary Movies of *pi3k1/2*-null cells in the presence or absence of LY294002 are available online.

[a] Applied concentration; in the small population assay, the cAMP concentration around the cell is about two- to fivefold lower.

[b] In the pipette assay, the concentration around the cell is 50–200 nM cAMP. ND, not determined.

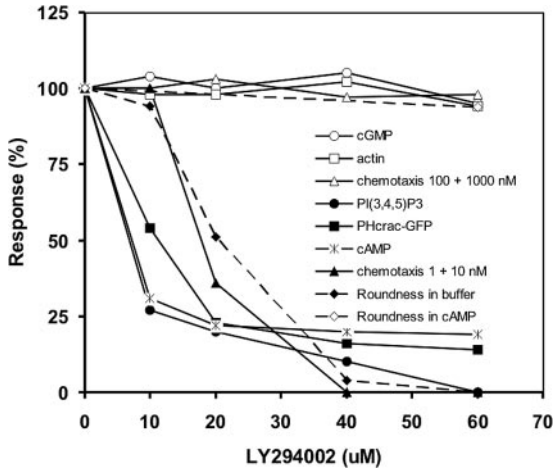

Figure 9. Summary of effects of LY294002. The chemoattractant cAMP induces several responses in *Dictyostelium*, which were measured at different concentrations of the PI3-kinase inhibitor LY294002. The response in the absence of LY294002 was set at 100% (see Figures 1–8 and Tables 1 and 2 for primary data). Some responses are inhibited by LY294002 (with half-maximal inhibition IC_{50} in parentheses): PI(3,4,5)P_3 production (IC_{50} = 6 μM), cAMP production (IC_{50} = 5 μM), PHcrac-GFP translocation (IC_{50} = 11 μM), and chemotaxis at low (1 and 10 nM) cAMP concentrations (IC_{50} = 17 μM). Other responses are not significantly inhibited by 60 μM LY294002: cGMP response, initial F-actin response, and chemotaxis at high (100 and 1000 nM) cAMP concentrations. The dashed lines show the effect of LY294002 on the roundness of cells stimulated with 500 nM cAMP (no inhibition) and of cells not stimulated with cAMP (IC_{50} = 20 μM; the roundness was set at 100% in the absence of LY294002 and at 0% in the presence of 60 μM LY294002).

and the TOR complex (Lee *et al.*, 2005). Although defective CRAC translocation to PI(3,4,5)P_3 in the membrane is probably the main cause of reduced cAMP accumulation in cells with inhibited PI3K signaling, the other signaling components may also depend on PI3K signaling and contribute to the effects observed. More experiments are required to understand the different effects of genetic inactivation of PI3K and pharmacological inhibition of PI3K on the late cAMP response and adaptation of ACA.

Aggregation of LY294002 treated cells is strongly inhibited, most likely due to this inhibition of cAMP production by LY294002. The presence of residual cAMP production may explain that aggregation does occur after a significant delay. The cAMP amounts are apparently high enough to form small aggregation centers at low frequency. Once a stable aggregation center has formed, enough cAMP is produced to induce cell polarity and chemotaxis for aggregation to proceed.

The Function of PI(3,4,5)P_3 in Cell Polarity and Chemotaxis

In the presence of LY294002, cells do not polarize, although pseudopod formation is still possible. Addition of cAMP restores cell polarity with half-maximal effect at 15 nM cAMP and a half-time of 2–3 min. One possibility is that PI(3,4,5)P_3 is essential for cell polarity, in which case PI(3,4,5)P_3 levels are below the threshold for polarity in LY294002-treated cells, whereas in cAMP-stimulated cells the small increase of PI(3,4,5)P_3 levels surpasses the threshold. Alternatively, the inhibition of cell polarity by LY294002 may be due to the inhibition of cAMP production, since starved *aca*$^-$ cells also do not polarize in the absence of cAMP, but become polarized in the presence of externally provided cAMP, suggesting that cAMP is necessary for cell polarization (Kriebel *et al.*, 2003). The LY294002-treated round cells have a very low chemotaxis index toward low cAMP concentrations that do not yet induce cell polarity (1 and 10 nM cAMP in the small population assay). In addition, chemotaxis toward higher cAMP concentrations (100 and 1000 nM cAMP) is also low as long as cells are still round, but become essentially normal after cAMP has induced cell polarity. These results suggest that the inhibition of chemotaxis by LY294002 is due to the inhibition of cell polarity and not to inhibition of directional sensing. It might be argued that LY294002-treated wild-type cells still produce some PI(3,4,5)P_3, although undetectable, that is sufficient to allow a chemotactic response. Therefore, we have tested chemotaxis in *pi3k1/2*-null cells in the presence of LY294002. These cells do not have a detectable activation of ACA, which is a very sensitive indicator for PI3K activity. In contrast to published data (Funamoto *et al.*, 2001, 2002), we observed essentially normal chemotaxis index in *pi3k1/2*-null cells, even in the presence of 60 μM LY294002. Thus at the most stringent condition of PI3K inhibition, cells exhibit an efficient directional chemotactic response. Despite good orientation of LY294002-treated cells in a cAMP gradient, the speed of cell movement is significantly reduced. The effect of LY294002 on the speed of locomotion in cAMP gradients is much larger for *pi3k1/2*-null cells (66 ± 18% reduction) than for wild-type cells (26 ± 4% reduction). Furthermore, wild-type cells and *pi3k1/2*-null cells move at approximately the same speed in buffer (unpublished data) and in cAMP gradients (Table 2), suggesting that the speed of locomotion is affected only at severe inhibition of PI3K signaling.

Although PI(3,4,5)P_3 may not be essential for directional sensing, many observations strongly suggest that PI(3,4,5)P_3, when present, affects F-actin and pseudopod formation. Cells with a deletion of *pten* exhibit a broad localization of PHcrac-GFP and F-actin, which is associated with many protrusion at a broad leading edge. When *pten*-null cells are stimulated with cAMP, the first phase of actin polymerization is unaffected compared with wild-type cells but the second phase is dramatically enhanced. Furthermore, in uniformly stimulated control cells, PHcrac-GFP patches are formed at smooth concave areas of the cell; subsequently, the first pseudopod is always formed at the position of the PHcrac-GFP patch. The broad localization of PHcrac-GFP in *pten*-null cells is associated with impaired chemotaxis. Interestingly, inhibition PI3-kinase activity in *pten*-null cells by LY294002 eliminated the second peak of actin polymerization and largely restored the chemotaxis defect of these cells (Chen *et al.*, 2003). These previous and present experiments suggest that uncontrolled high PI(3,4,5)P_3 levels inhibits chemotaxis, whereas severe reduction of PI(3,4,5)P_3 levels has little effect on directional sensing.

The function of PI3K signaling in natural cAMP waves during cell aggregation is probably complex. In wild-type cells cAMP waves are produced every 6 min with cAMP concentrations below 10 nM in the troughs and ~1 μM at the top of the wave (Tomchik and Devreotes, 1981). Chemotaxis occurs during the period of increasing cAMP concentration, which lasts for ~90 s. We define chemotactic movement as the distance a cell has moved in the direction of the cAMP gradient per unit of time, which is the product of chemotaxis index and speed. With LY294002-inhibited PI3K it is expected that cell aggregation and chemotactic movement in natural cAMP gradient waves will be reduced because 1) cAMP relay is partly inhibited and the cAMP wave will

consequently have different kinetic properties; 2) cells have reduced speed of movement at all cAMP concentrations; and 3) at low cAMP concentrations (<100 nM), cells are round and chemotactic movement is inhibited; in wild-type cells the cAMP concentration reaches a concentration of ~100 nM at 10–15 s after the onset of the cAMP wave; and 4) at higher cAMP concentrations, chemotactic movement is reduced because PI3K-inhibited cells need to become elongated before they exhibit good chemotaxis, which may require a significant portion of the residual 75 s rising flank of the cAMP wave. Taken together, PI3K signaling is a crucial component of the *Dictyostelium* aggregation chemotactic machinery, with predominant roles in cell speed, cell polarity, and cAMP gradient formation and a minor role in gradient detection.

ACKNOWLEDGMENTS

We thank Ruchira Engel for her support in obtaining confocal images. This work was supported by The Netherlands Organization of Scientific Research.

REFERENCES

Bosgraaf, L., Russcher, H., Smith, J. L., Wessels, D., Soll, D. R., and Van Haastert, P.J.M. (2002). A novel cGMP-signaling pathway mediating myosin phosphorylation and chemotaxis in *Dictyostelium.* EMBO J. *21*, 4560–4570.

Bosgraaf, L., and Van Haastert, P. J. (2002). A model for cGMP signal transduction in *Dictyostelium* in perspective of 25 years of cGMP research. J. Muscle Res. Cell Motil. *23*, 781–791.

Chen, L., Janetopoulos, C., Huang, Y. E., Iijima, M., Borleis, J., and Devreotes, P. N. (2003). Two phases of actin polymerization display different dependencies on PI(3,4,5)P3 accumulation and have unique roles during chemotaxis. Mol. Biol. Cell *14*, 5028–5037.

Comer, F. I., and Parent, C. A. (2006). Phosphoinositide 3-kinase activity controls the chemoattractant-mediated activation and adaptation of adenylyl cyclase. Mol. Biol. Cell *17*, 357–366.

Devreotes, P., and Janetopoulos, C. (2003). Eukaryotic chemotaxis: distinctions between directional sensing and polarization. J. Biol. Chem. *278*, 20445–20448.

Dormann, D., Weijer, G., Dowler, S., and Weijer, C. J. (2004). In vivo analysis of 3-phosphoinositide dynamics during *Dictyostelium* phagocytosis and chemotaxis. J. Cell Sci. *117*, 6497–6509.

Funamoto, S., Meili, R., Lee, S., Parry, L., and Firtel, R. A. (2002). Spatial and temporal regulation of 3-phosphoinositides by PI 3-kinase and PTEN mediates chemotaxis. Cell *109*, 611–623.

Funamoto, S., Milan, K., Meili, R., and Firtel, R. A. (2001). Role of phosphatidylinositol 3′ kinase and a downstream pleckstrin homology domain-containing protein in controlling chemotaxis in dictyostelium. J. Cell Biol. *153*, 795–810.

Huang, Y. E., Iijima, M., Parent, C. A., Funamoto, S., Firtel, R. A., and Devreotes, P. N. (2003). Receptor mediated regulation of PI3Ks confines PI(3,4,5)P3 to the leading edge of chemotaxing cells. Mol. Biol. Cell *14*, 1913–1922.

Iijima, M., and Devreotes, P. (2002). Tumor suppressor PTEN mediates sensing of chemoattractant gradients. Cell *109*, 599–610.

Iijima, M., Huang, Y. E., Luo, H. R., Vazquez, F., and Devreotes, P. N. (2004). Novel mechanism of PTEN regulation by its PIP2 binding motif is critical for chemotaxis. J. Biol. Chem. *279*, 16606–16613.

Insall, R., Kuspa, A., Lilly, P. J., Shaulsky, G., Levin, L. R., Loomis, W. F., and Devreotes, P. (1994). CRAC, a cytosolic protein containing a pleckstrin homology domain, is required for receptor and G protein-mediated activation of adenylyl cyclase in *Dictyostelium*. J. Cell Biol. *126*, 1537–1545.

Janetopoulos, C., Borleis, J., Vazquez, F., Iijima, M., and Devreotes, P. (2005). Temporal and spatial regulation of phosphoinositide signaling mediates cytokinesis. Dev. Cell *8*, 467–477.

Janetopoulos, C., Ma, L., Devreotes, P. N., and Iglesias, P. A. (2004). Chemoattractant-induced phosphatidylinositol 3,4,5-trisphosphate accumulation is spatially amplified and adapts, independent of the actin cytoskeleton. Proc. Natl. Acad. Sci. USA *101*, 8951–8956.

Konijn, T. M. (1970). Microbiological assay of cyclic 3′,5′-AMP. Experientia *26*, 367–369.

Kriebel, P. W., Barr, V. A., and Parent, C. A. (2003). Adenylyl cyclase localization regulates streaming during chemotaxis. Cell *112*, 549–560.

Lee, S., Comer, F. I., Sasaki, A., McLeod, I. X., Duong, Y., Okumura, K., Yates, J. R., 3rd, Parent, C. A., and Firtel, R. A. (2005). TOR Complex 2 integrates cell movement during chemotaxis and signal relay in *Dictyostelium.* Mol. Biol. Cell *16*, 4572–4583.

Li, Z. *et al.* (2003). Directional sensing requires G beta gamma-mediated PAK1 and PIX alpha-dependent activation of Cdc42. Cell *114*, 215–227.

Loovers, H. M., Veenstra, K., Snippe, H., Pesesse, X., Erneux, C., and van Haastert, P. J. (2003). A diverse family of inositol 5-phosphatases playing a role in growth and development in *Dictyostelium discoideum.* J. Biol. Chem. *278*, 5652–5658.

Mato, J. M., Losada, A., Nanjundiah, V., and Konijn, T. M. (1975). Signal input for a chemotactic response in the cellular slime mold *Dictyostelium discoideum.* Proc. Natl. Acad. Sci. USA *72*, 4991–4993.

Parent, C. A. (2004). Making all the right moves: chemotaxis in neutrophils and *Dictyostelium*. Curr. Opin. Cell Biol. *16*, 4–13.

Parent, C. A., Blacklock, B. J., Froehlich, W. M., Murphy, D. B., and Devreotes, P. N. (1998). G protein signaling events are activated at the leading edge of chemotactic cells. Cell *95*, 81–91.

Parent, C. A., and Devreotes, P. N. (1999). A cell's sense of direction. Science *284*, 765–770.

Pitt, G. S., Milona, N., Borleis, J., Lin, K. C., Reed, R. R., and Devreotes, P. N. (1992). Structurally distinct and stage-specific adenylyl cyclase genes play different roles in *Dictyostelium* development. Cell *69*, 305–315.

Postma, M., Roelofs, J., Goedhart, J., Gadella, T.W.J., Visser, A.J.W.G., and Van Haastert, P.J.M. (2003). Uniform cAMP stimulation of *Dictyostelium* cells induces localized patches of signal transduction and pseudopodia. Mol. Biol. Cell *14*, 5019–5027.

Postma, M., Roelofs, J., Goedhart, J., Loovers, H. M., Visser, A.J.W.G., and Van Haastert, P.J.M. (2004). Sensitisation of *Dictyostelium* chemotaxis by PI3-kinase mediated self-organising signalling patches. J. Cell Sci. *117*, 2925–2935.

Potma, E., de Boeij, W. P., van Haastert, P. J., and Wiersma, D. A. (2001). Real-time visualization of intracellular hydrodynamics in single living cells. Proc. Natl. Acad. Sci. USA *98*, 1577–1582.

Saran, S., Meima, M. E., Alvarez-Curto, E., Weening, K. E., Rozen, D. E., and Schaap, P. (2002). cAMP signaling in *Dictyostelium.* Complexity of cAMP synthesis, degradation and detection. J. Muscle Res. Cell Motil. *23*, 793–802.

Sasaki, A. T., Chun, C., Takeda, K., and Firtel, R. A. (2004). Localized Ras signaling at the leading edge regulates PI3K, cell polarity, and directional cell movement. J. Cell Biol. *167*, 505–518.

Snaar-Jagalska, B. E., and Van Haastert, P. J. (1994). G-protein assays in *Dictyostelium.* Methods Enzymol. *237*, 387–408.

Soll, D. R. (1999). Computer-assisted three-dimensional reconstruction and motion analysis of living, crawling cells. Comput. Med. Imaging Graph. *23*, 3–14.

Tomchik, K. J., and Devreotes, P. N. (1981). Adenosine 3′,5′-monophosphate waves in *Dictyostelium discoideum*: a demonstration by isotope dilution-fluorography. Science *212*, 443–446.

Wang, F., Herzmark, P., Weiner, O. D., Srinivasan, S., Servant, G., and Bourne, H. R. (2002). Lipid products of PI(3)Ks maintain persistent cell polarity and directed motility in neutrophils. Nat. Cell Biol. *4*, 513–518.

Weiner, O. D., Neilsen, P. O., Prestwich, G. D., Kirschner, M. W., Cantley, L. C., and Bourne, H. R. (2002). A PtdInsP(3)- and Rho GTPase-mediated positive feedback loop regulates neutrophil polarity. Nat. Cell Biol. *4*, 509–513.

Xu, J., Wang, F., Van Keymeulen, A., Herzmark, P., Straight, A., Kelly, K., Takuwa, Y., Sugimoto, N., Mitchison, T., and Bourne, H. R. (2003). Divergent signals and cytoskeletal assemblies regulate self-organizing polarity in neutrophils. Cell *114*, 201–214.

Zhou, K., Pandol, S., Bokoch, G., and Traynor-Kaplan, A. E. (1998). Disruption of *Dictyostelium* PI3K genes reduces [^{32}P]phosphatidylinositol 3,4 bisphosphate and [^{32}P]phosphatidylinositol trisphosphate levels, alters F-actin distribution and impairs pinocytosis. J. Cell Sci. *111*(Pt 2), 283–294.

Zhou, K., Takegawa, K., Emr, S. D., and Firtel, R. A. (1995). A phosphatidylinositol (PI) kinase gene family in *Dictyostelium discoideum*: biological roles of putative mammalian p110 and yeast Vps34p PI 3-kinase homologs during growth and development. Mol. Cell Biol. *15*, 5645–5656.